

# Audio-Visual Speech Enhancement Based on Multimodal Deep Convolutional Neural Networks

Jen-Cheng Hou, Syu-Siang Wang, Ying-Hui Lai, Yu Tsao, *Member, IEEE*,  
Hsiu-Wen Chang, and Hsin-Min Wang, *Senior Member, IEEE*

**Abstract**—Speech enhancement (SE) aims to reduce noise in speech signals. Most SE techniques focus on addressing audio information only. In this work, inspired by multimodal learning, which utilizes data from different modalities, and the recent success of convolutional neural networks (CNNs) in SE, we propose an audio-visual deep CNNs (AVDCNN) SE model, which incorporates audio and visual streams into a unified network model. We also propose a multi-task learning framework for reconstructing audio and visual signals at the output layer. Precisely speaking, the proposed AVDCNN model is structured as an audio-visual encoder-decoder network, in which audio and visual data are first processed using individual CNNs, and then, fused into a joint network to generate enhanced speech (the primary task) and reconstructed image (the secondary task) at the output layer. It is trained in an end-to-end manner, and parameters are jointly learned through back-propagation. We evaluate enhanced speech using five instrumental criteria. Results show that the AVDCNN model yields notably better performance, compared with an audio-only CNN-based SE model and two conventional SE approaches, confirming the effectiveness of integrating visual information into the SE process. In addition, the AVDCNN model also outperforms an existing audio-visual SE model, confirming its capability of effectively combining audio and visual information in SE.

**Index Terms**—Audio-visual systems, deep convolutional neural networks, multimodal learning, speech enhancement.

## I. INTRODUCTION

The primary goal of speech enhancement (SE) is to improve

Copyright (c) 2016 IEEE. Personal use of this material is permitted. However, permission to use this material for any other purposes must be obtained from the IEEE by [pubs-permissions@ieee.org](mailto:pubs-permissions@ieee.org).

Jen-Cheng Hou is with the Research Center for Information Technology Innovation at Academia Sinica, Taipei, Taiwan. (email:coolkiu@citi.sinica.edu.tw).

Syu-Siang Wang is with the Graduate Institute of Communication Engineering, National Taiwan University, Taipei, Taiwan. (email:d02942007@ntu.edu.tw).

Ying-Hui Lai is with Department of Electrical Engineering, Yuan Ze University, Taoyuan, Taiwan. (email: yhlai@ee.yzu.edu.tw).

Yu Tsao is with the Research Center for Information Technology Innovation at Academia Sinica, Taipei, Taiwan. (email:yu.tsao@citi.sinica.edu.tw).

Hsiu-Wen Chang is with Department of Audiology and Speech language pathology, Mackay Medical College, New Taipei City, Taiwan. (email:hsiuwen@mmc.edu.tw).

Hsin-Min Wang is with the Institute of Information Science at Academia Sinica, Taipei, Taiwan. (email:whm@iis.sinica.edu.tw).

the intelligibility and quality of noisy speech signals by reducing the noise components of noise-corrupted speech. To attain satisfactory performance, SE has been used as a fundamental unit in various speech-related applications, such as automatic speech recognition [1, 2], speaker recognition [3, 4], speech coding [5, 6], hearing aids [7, 8], and cochlear implant [9, 10]. In the past few decades, numerous SE methods have been proposed and proven to provide improved sound quality. One notable approach, i.e., spectral restoration, estimates a gain function (based on the statistics of noise and speech components), which is then used to suppress noise components in the frequency domain to obtain a clean speech spectrum from a noisy speech spectrum [11–15]. Another class of approaches adopts a nonlinear model to map noisy to clean speech signals [16–19]. In recent years, SE methods based on deep learning have been proposed and investigated extensively, such as a denoising autoencoder [20, 21]. SE methods using deep neural networks (DNNs) generally exhibit better performance than conventional SE models [22–24]. Approaches that utilize the recurrent neural networks (RNNs) and long short-term memory (LSTM) models have also been confirmed to show promising SE and related speech signal processing performances [25–28]. In addition, inspired by the success of image recognition using convolutional neural networks (CNNs), a CNN-based model has been shown to obtain good results in SE owing to its strength in handling the image-like 2-D time-frequency representation of noisy speech [29, 30].

In addition to speech signals, visual information is important in human-human or human-machine interaction. A study of the McGurk effect [31] indicated that the shape of the mouth or lips could play an important role in speech processing. Accordingly, audio-visual multimodality has been adopted in numerous fields of speech-processing [32–37]. These results showed that visual modality enhances the performance of speech processing, compared with its counterpart that uses audio modality alone. In addition, topics about fusing audio and visual features were addressed in [38, 39], in which additional reliability measures were used for better dynamic weighting of audio and visual streams. On the other hand, as studies shown in [40, 41], intuitive fusion schemes were adopted in multimodal learning based on the architectures of neural networks. In the area of audio-visual SE, there were also several related works [42–48]. Most of them were based on an enhancement filter with the help of

hand-crafted visual features from lip shape information. Recently, audio-visual SE models based on deep learning have also been proposed [49, 51]. In [49], Mel filter banks and the Gauss-Newton deformable part model [50] were used to extract audio and mouth shape features. Experimental results showed that DNNs with audio-visual inputs outperformed DNNs with only audio inputs in several standardized instrumental evaluations. In [51], the authors proposed to deal with audio and visual data by DNNs and CNNs, respectively. The noisy audio features and the corresponding video features were used as the input, and the audio features were used as the target during training.

In the present work, we adopt CNNs to process both audio and visual streams. The outputs of the two networks are fused into a joint network. Noisy speech and visual data are placed at inputs, and clean speech and visual data are placed at outputs. The entire model is trained in an end-to-end manner and structured as an audio-visual encoder-decoder network. Notably, the visual information at the output layer serves as a part of the constraints during the training of the model, and thus, the system adopts a multi-task learning scheme that considers heterogeneous information. Such a unique audio-visual encoder-decoder network design has not been used in related works [49, 51]. In short, the proposed audio-visual SE model takes the advantage of CNNs, which have shown effective in speech enhancement [29, 30] and image and face recognition [52, 53], for both audio and visual streams, and the properties of deep learning, i.e., reducing human-engineering efforts by end-to-end learning and intuitive fusion schemes in multi-modal learning tasks. To our best knowledge, this is the first model exploits all the aforementioned properties at once in a deep learning-based audio-visual SE model.

Our experimental results show that the proposed audio-visual SE model outperforms three audio-only baseline models in terms of several standard evaluation metrics, including perceptual evaluation of speech quality (PESQ) [54], short-time objective intelligibility (STOI) [55], speech distortion index (SDI) [56], hearing-aid speech quality index (HASQI) [57], and hearing-aid speech perception index (HASPI) [58], confirming the effectiveness of incorporating visual information into the CNN-based multimodal SE framework. Besides, compared with the audio-visual SE model in [49], our model obtains better performance in the experimental results, showing that our model is more effective in combining audio and visual information in SE. An alternative fusion scheme (i.e., early fusion) based on our audio-visual model is also evaluated and the results show that the proposed architecture is better than the early fusion one.

The rest of this paper is organized as follows: Section II describes the preprocessing of audio and visual streams. Section III introduces the proposed CNN-based audio-visual model for SE and describes three baseline models for comparison. Section IV describes the experimental setup and results, and discussion is followed in Section V. Section VI provides the concluding remarks of this study.

## II. DATASET AND PREPROCESSING

In this section, we provide the details of datasets and preprocessing for audio and visual streams.

### A. Data Collection

The prepared dataset contains video recordings of 320 utterances of Mandarin sentences spoken by a native speaker. The script for recording is based on the Taiwanese Mandarin Chinese version of the hearing in noise test (Taiwan MHINT) [59]. The script was made by native speakers and each sentence contains 10 Chinese characters with phoneme designed to distribute equally. The length of each utterance is approximately 3–4 seconds. The utterances were recorded in a quiet room with sufficient light, and the speaker was filmed from the front view. Videos were recorded at 30 frames per second (fps) at a resolution of 1920 pixels  $\times$  1080 pixels. Stereo audio channels were recorded at 48 kHz. Three-fourths of the corpus (280 utterances) were randomly selected as a training set, with the remaining 40 utterances used as the testing set.

### B. Audio Feature Extraction

We resampled the audio signal at 16 kHz and used only a mono channel for further processing. Speech signals were converted into the frequency domain and processed into a sequence of frames using the short-time Fourier transform. Each frame was windowed by 32 milliseconds, and the window overlap ratio was 37.5%. For each speech frame, we extracted the logarithmic power spectrum and normalized the value by removing the mean and dividing by the standard deviation. The normalization was conducted per window. We concatenated  $\pm 2$  frames to the central frame as the context windows. Accordingly, audio features had dimensions of  $257 \times 5$  at each time step. We use  $X$  and  $Y$  to denote noisy and clean speech features, respectively.

### C. Visual Feature Extraction

For the visual stream, we converted each video, which contained an utterance, into image sequences at a fixed frame rate of 50 fps. Next, we detected the mouth using the Viola–Jones method [60], resized the cropped mouth region to 16 pixels  $\times$  24 pixels, and retained its RGB channels. In each channel, we rescaled image pixel intensities in a range of 0 to 1. We subtracted the mean and divided it by the standard deviation for normalization. The normalization was conducted per colored mouth image. In addition, we concatenated  $\pm 2$  frames to the central frame, resulting in visual features having dimensions of  $80 \times 24 \times 3$  at each time step. We use  $Z$  to represent input visual features. For each utterance, the number of frames of audio spectrum and the number of mouth images were made the same by truncation if needed.

## III. AUDIO-VISUAL DEEP CONVOLUTIONAL NEURAL NETWORKS (AVDCNN)

The architecture of the proposed AVDCNN model is shown in Fig. 1. It is composed of two individual networks that handle audio and visual streams, namely Audio Network and Visual Network. The outputs of two networks are fused into another network, called Fusion Network. The CNN, maximum pooling

layer, and fully-connected layer in the diagram are abbreviated as  $\text{Conv}_{a1}$ ,  $\text{Conv}_{a2}$ ,  $\text{Conv}_{v1}$ , ...,  $\text{Pool}_{a1}$ ,  $\text{FC1}$ ,  $\text{FC2}$ ,  $\text{FC}_{a3}$ , and  $\text{FC}_{v3}$ , where subscripts ‘a’ and ‘v’ denote the audio and visual stream, respectively. In the following section, we describe the training procedure of the AVDCNN model.

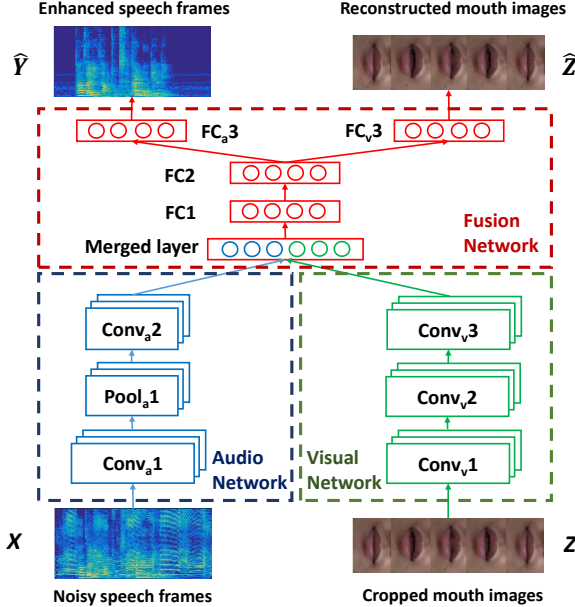


Fig. 1. Architecture of the proposed AVDCNN model.

#### A. Training the AVDCNN Model

To train the AVDCNN model, we first prepare noisy-clean speech pairs and mouth images. As described in parts B and C in Section II, we have the logarithmic amplitudes of noisy ( $X$ ) and clean ( $Y$ ) spectra and the corresponding visual features ( $Z$ ). For each time step, we obtain the output of Audio Network as

$$A_i = \text{Conv}_{a2}(\text{Pool}_{a1}(\text{Conv}_{a1}(X_i))), i = 1 \dots K \quad (1)$$

where  $K$  is the number of training samples. The output of Visual Network is

$$V_i = \text{Conv}_{v3}(\text{Conv}_{v2}(\text{Conv}_{v1}(Z_i))), i = 1 \dots K \quad (2)$$

Next, we flatten  $A_i$  and  $V_i$ , and concatenate the two features as the input of Fusion Network,  $F_i = [A_i' \ V_i']'$ . A feed-forward cascaded fully-connected network is computed as:

$$\hat{Y}_i = \text{FC}_{a3}(\text{FC}_2(\text{FC}_1(F_i))), i = 1 \dots K \quad (3)$$

$$\hat{Z}_i = \text{FC}_{v3}(\text{FC}_2(\text{FC}_1(F_i))), i = 1 \dots K \quad (4)$$

The parameters of the AVDCNN model, denoted as  $\theta$ , are randomly initialized from -1 to 1, and are trained by optimizing the following objective function using back-propagation:

$$\min_{\theta} \left( \frac{1}{K} \sum_{i=1}^K \|\hat{Y}_i - Y_i\|_2^2 + \mu \|\hat{Z}_i - Z_i\|_2^2 \right), \quad (5)$$

where  $\mu$  is a mixing weight.

Stride size of  $1 \times 1$  is used in the CNNs of the AVDCNN model, and a dropout of 0.1 is adopted after  $\text{FC1}$  and  $\text{FC2}$  to prevent overfitting. Batch normalization is applied for each layer in the model. Other configurations are shown in Table I.

#### B. Using the AVDCNN Model for Speech Enhancement

In the testing phase, the logarithmic amplitudes of noisy speech signals and the corresponding visual features are fed into the trained AVDCNN model to obtain the logarithmic amplitudes of enhanced speech signals and the visual features as outputs. Similar to spectral restoration approaches, the phases of noisy speech are borrowed as the phases for enhanced speech. Then, the AVDCNN-enhanced amplitudes and phase information are used to synthesize enhanced speech. We consider the visual features at the output of the trained AVDCNN model only as auxiliary information. This special design enables the AVDCNN model to process audio and visual information at the same time. Thus, the training process is done in a multi-task learning manner, which has been proven to achieve better performance than single-task learning in several tasks [61, 62].

#### C. Baseline Models

In this work, we compare the proposed AVDCNN model with three audio-only baseline models. The first is the audio-only deep CNNs (ADCNN) model. As shown in Fig. 2, the ADCNN model disconnects all visual-related parts in the AVDCNN model (cf. Fig. 1), and keeps the remaining configurations. The second and third are two conventional SE approaches, namely Karhunen-Loéve transform (KLT) [63] and log minimum mean squared error (logMMSE) [64, 65].

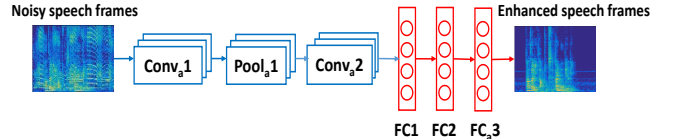


Fig. 2. Architecture of the ADCNN model, which is the same as the AVDCNN model in Fig. 1 with visual parts disconnected.

TABLE I  
CONFIGURATIONS OF THE AVDCNN MODEL

Layer Name	Kernel	Activation Function	Number of Filters or Neurons
Conv <sub>a1</sub>	$12 \times 2$	Linear	10
Pool <sub>a1</sub>	$2 \times 1$		
Conv <sub>a2</sub>	$5 \times 1$	Linear	4
Conv <sub>v1</sub>	$15 \times 2$	Linear	12
Conv <sub>v2</sub>	$7 \times 2$	Linear	10
Conv <sub>v3</sub>	$3 \times 2$	Linear	6
Merged Layer			2804
FC1		Sigmoid	1000
FC2		Sigmoid	800
FC <sub>a3</sub>		Linear	600
FC <sub>v3</sub>		Linear	1500

## IV. EXPERIMENTS AND RESULTS

#### A. Experimental Setup

In this section, we describe the experimental setup for the speech enhancement task in this study. To prepare the clean-noisy speech pairs, we follow the concept in a previous study

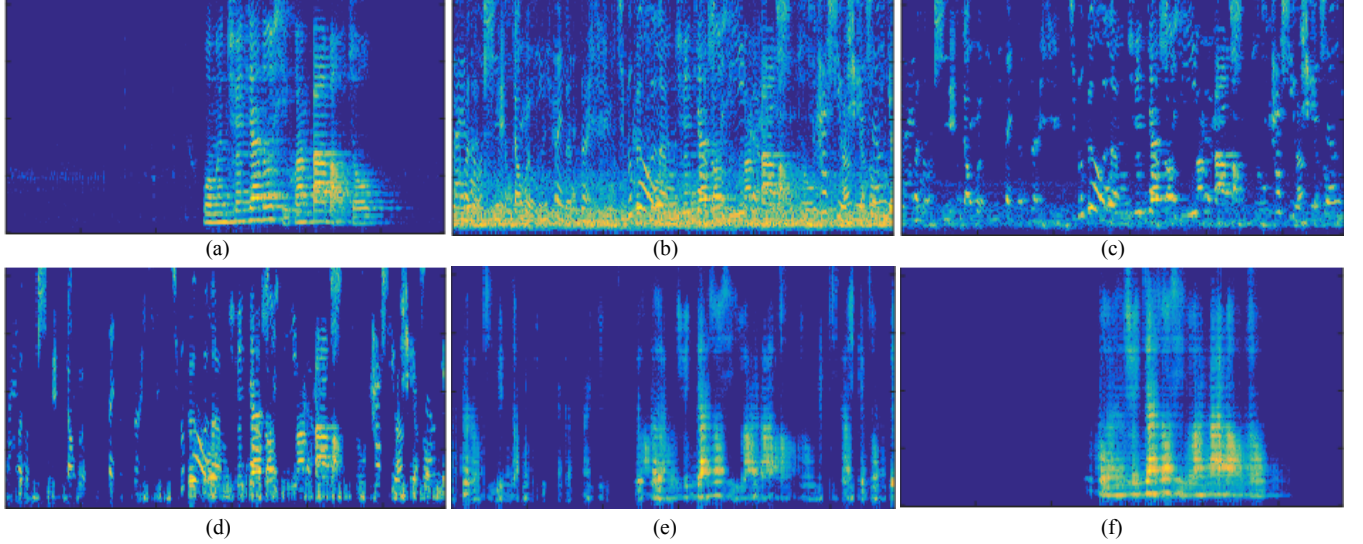


Fig. 3 Comparison of spectrograms: (a) clean speech, (b) noisy speech of 2T(on-air) at -5dB SIR with ambient noise at -5dB SAR, (c) speech enhanced by logMMSE, (d) speech enhanced by KLT, (e) speech enhanced by ADCNN, and (f) speech enhanced by AVDCNN.

[66], where the effects of both interference noise and ambient noise were considered. For the training set, we used 91 different noise types as interference noises. These 91 noises were a subset of the 104 noise types used in [67, 68]. 13 noise types that were similar to the test noise types were removed. The car engine noises under 5 driving conditions were used to form the ambient noise set, including engine idling, 35mph with the windows up, 35mph with the windows down, 55mph with the windows up, and 55mph with the windows down. The car engine noises were excerpted from the AVICAR dataset [69]. We concatenated these car noises to form our final ambient noise source for training. To form the training set, we first randomly chose 280 out of 320 clean utterances. The clean utterances were artificially mixed with 91 noise types at 10dB, 6dB, 2dB, -2dB, -6dB signal-to-interference noise ratios (SIRs) and the ambient noise at the 10dB, 6dB, 2dB, -2dB, -6dB signal-to-ambient noise ratios (SARs), resulting in a total of  $(280 \times 91 \times 5 \times 5)$  utterances.

Next, to form the testing set, we adopted 10 types of interference noises, including baby crying, pure music, music with lyrics, siren, one background talker (1T), two background talkers (2T), and three background talkers (3T), where for 1T, 2T, and 3T background talker noises, there were two modes: on-air recording and room recording. These noises were unseen in the training set, i.e., a noise-mismatched condition, and were particularly chosen because we intended to simulate the car-driving condition as our test scenario. In addition, the ambient noise for testing was 60 mph car engine noise excerpted from the dataset used in [70], which was also different from the ones used in the training set. Consequently, for testing, there were 40 clean utterances, mixed with the 10 noise types at 5dB, 0dB, and -5dB SIRs, and one ambient noise at 5dB, 0dB, and -5dB SARs, resulting in a total of  $(40 \times 10 \times 3 \times 3)$  utterances. We used stochastic gradient descent and RMSprop [71] as the learning optimizer with an initial learning rate at 0.0001 to train the neural network model. We chose the weights of the model when the following 20 epochs exhibit improvements less than 0.1% in the training loss. The implementation was based on the Keras [72] library.

### B. Comparison of the Spectrogram

Fig. 3, (a), (b), (c), (d), (e), and (f) demonstrate the spectrograms of clean speech, noisy speech mixed with 2T (on-air) noise at -5dB SIR with -5dB SAR, and speech enhanced by the logMMSE, KLT, ADCNN, and AVDCNN methods, respectively. Since the designed condition is challenging, it is obvious that all the three audio-only SE approaches could not effectively remove the noise components. The phenomenon is especially obvious for the silence portion at the beginning of the utterance, where noise components can still be observed, even with ADCNN model (Fig. 3 (e)). On the contrary, with the help of auxiliary visual information, the AVDCNN model effectively suppressed the noise components in the parts when mouth was closed. In Section IV-A-G, we will show that the information from lip shape not only facilitated a more effective noise removal for non-speech parts but also increased the quality of enhanced speech in speech parts.

### C. Results of Instrumental Measures

In this section, we reported the results of four SE methods in terms of five instrumental metrics, including PESQ, STOI, SDI, HASQI, and HASPI. The PESQ measure (ranging from 0.5 to 4.5) indicates the quality measurement of enhanced speech. The STOI measure (ranging from 0 to 1) indicates the intelligibility measurement of enhanced speech. HASQI and HASPI measures (both ranging from 0 to 1) evaluate sound quality and perception, respectively, for both normal hearing and hearing-impaired people (by setting specific modes). In this study, the normal hearing mode was specified for both HASQI and HASPI measures. The SDI measure calculates the distortion measurement of clean and enhanced speech. Except for SDI, larger values indicate better performance. We reported the average evaluation score over the 40 test utterances under different noise type, SIR, and SAR conditions.

We first intended to investigate the SE performances on different noise types. Figs. 4-8, respectively, show the average

PESQ, STOI, SDI, HASQI, and HASPI scores of 10 different SIR noises and the enhanced speech obtained using different SE methods, where the SAR was fixed to 0dB. From Figs. 4-8, we first notice that the performances of two conventional SE methods (logMMSE and KLT) cannot effectively handle non-stationary noises. Next, when comparing the two CNN-based models, AVDCNN outperforms ADCNN consistently in terms of all evaluation metrics, confirming the effectiveness of the combination of visual and audio information to achieve better SE performance. To further confirm the significance of the improvement between the AVDCNN model and the second best system in each test condition in Figs 4-8, we performed the one-way analysis of variance (ANOVA) and Tukey post-hoc comparisons (TPHCs) [73]. The results confirmed that these scores differed significantly with p-values less than 0.05 in most conditions, except STOI (with music and siren noises), SDI (with baby crying, music, and siren noises), and HASPI (with music and siren noises). With a further analysis on the experimental results, we noted that among the 10 testing noise types, the evaluation scores of baby crying are always worse than those of other noise types, suggesting that the baby crying noise is relatively challenging to handle. Meanwhile, the multiple background talkers (2T, 3T) scenarios do not appear more challenging than that of the single background talker (1T).

Next, we compared the SE performances provided by different SE models on different SAR levels. Figs. 9-13 show the average PESQ, STOI, SDI, HASQI, and HASPI scores of noisy and the enhanced speech at specific SIR (over 10 different noise types) and SAR levels. In these figures, “ $\times$ ”, “ $\circ$ ”, “ $\square$ ” denote -5, 0, 5 dB SAR, respectively. Please note that a speech signal with a higher SAR indicates that it is involved with less car engine noise components. From Figs. 9-13, it is clear that: (1) the instrumental evaluation results of higher SAR levels are usually better than those of lower SAR levels; (2) AVDCNN outperforms other SE methods, especially more obvious in lower SIR levels; this result shows that visual information provides an important clue to assist SE in AVDCNN in very challenging conditions.

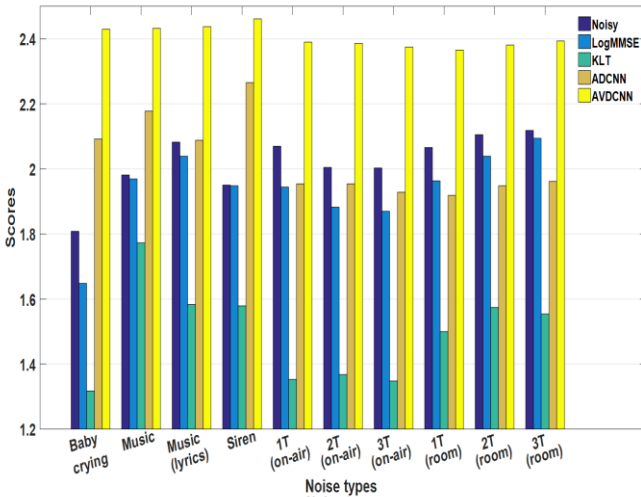


Fig. 4 Mean PESQ scores of 10 different noisy and their enhanced speech by different models over different SIRs at SAR 0dB.

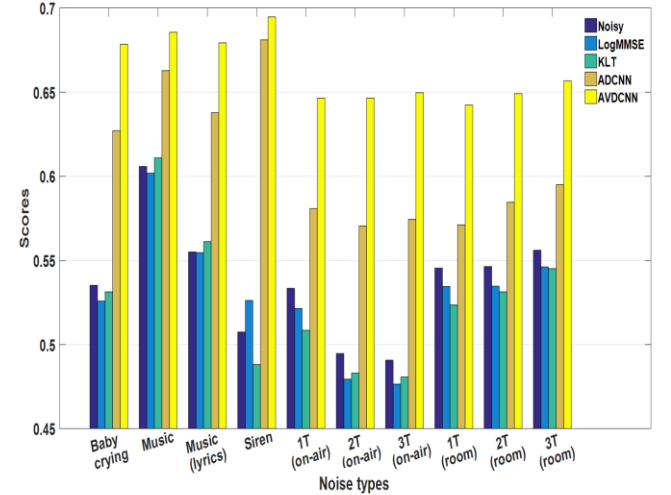


Fig. 5 Mean STOI scores of 10 different noisy and their enhanced speech by different models over different SIRs at SAR 0dB.

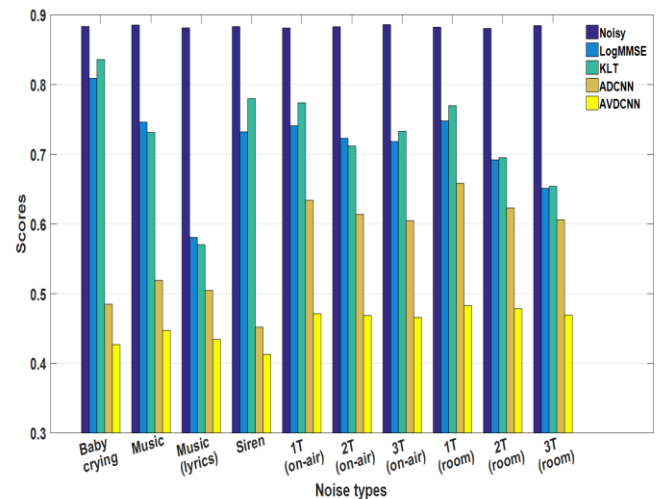


Fig. 6 Mean SDI scores of 10 different noisy and their enhanced speech by different models over different SIRs at SAR 0dB.

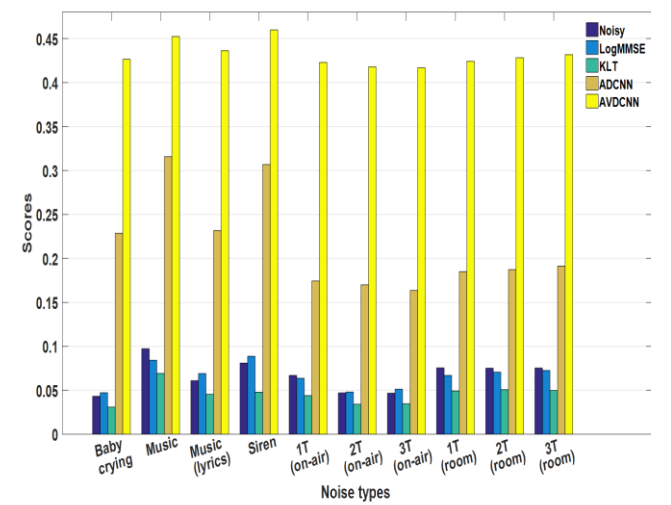


Fig. 7 Mean HASQI scores of 10 different noisy and their enhanced speech by different models over different SIRs at SAR 0dB.

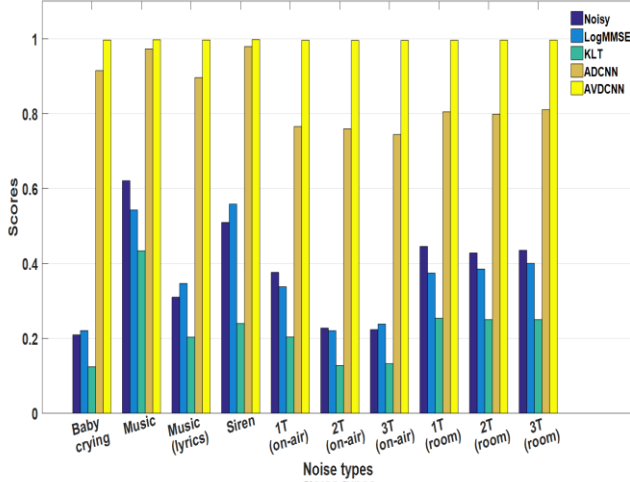


Fig. 8 Mean HASPI scores of 10 different noisy and their enhanced speech by different models over different SIRs at SAR 0dB.

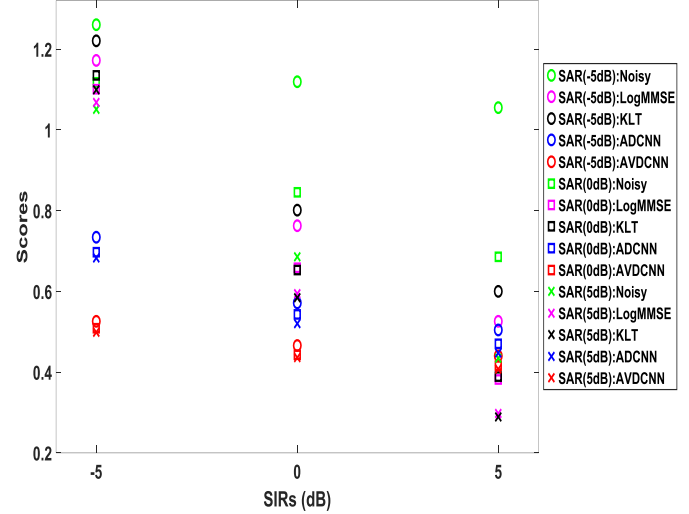


Fig. 11 Mean SDI over 10 noises at different SIRs for each SAR.

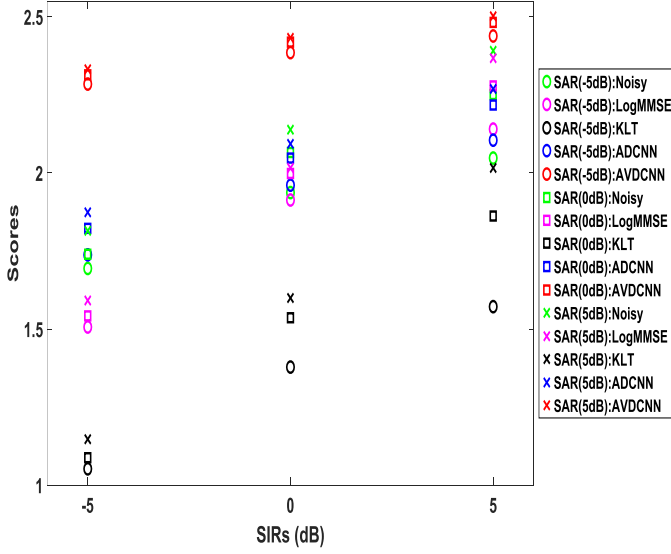


Fig. 9 Mean PESQ over 10 noises at different SIRs for each SAR.

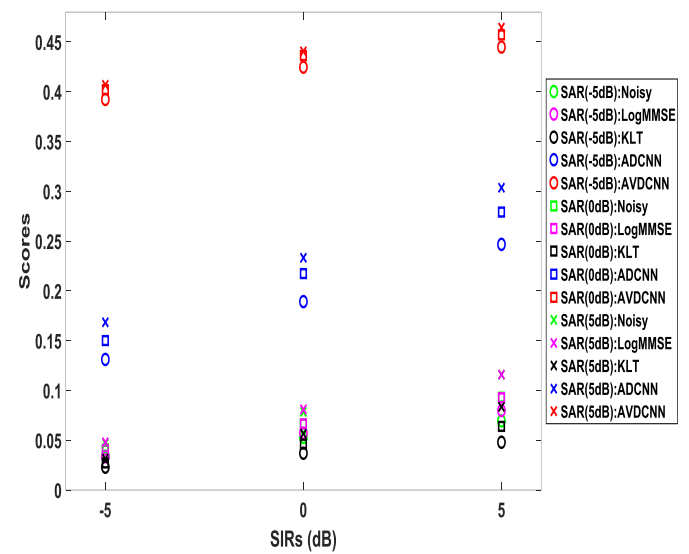


Fig. 12 Mean HASQI over 10 noises at different SIRs for each SAR.

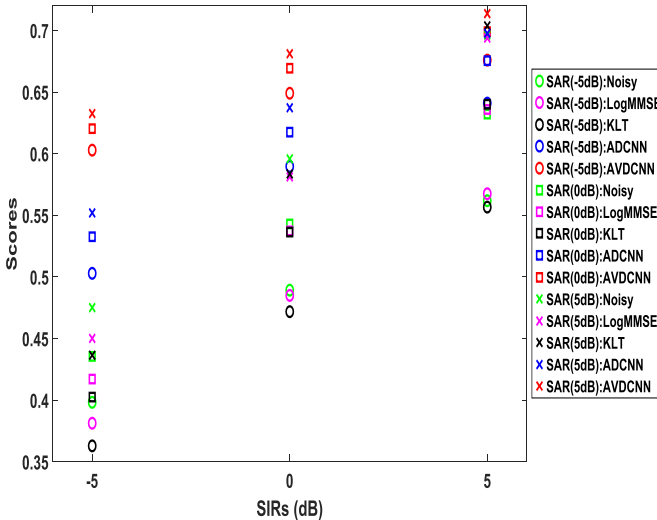


Fig. 10 Mean STOI over 10 noises at different SIRs for each SAR.

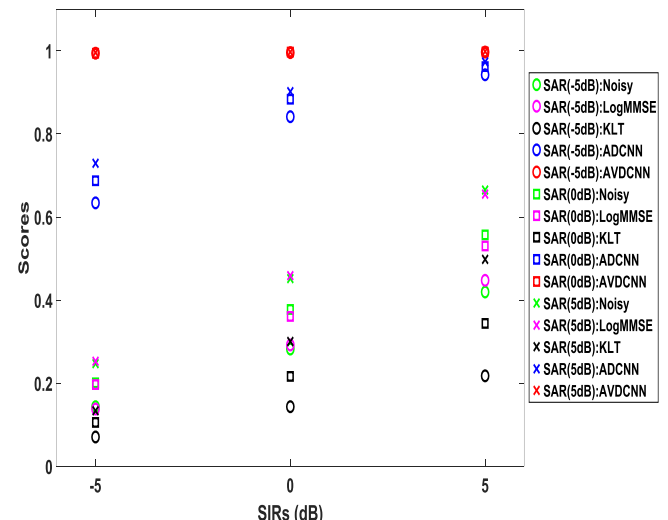


Fig. 13 Mean HASPI over 10 noises at different SIRs for each SAR.

#### D. Multi-style Training Strategy

A previous study [74] has shown that the input of a certain modality of a multimodal network could dominate over other input types. In our preliminary experiments, we observed similar properties. To alleviate this issue, we adopted the multi-style training strategy [75], which randomly selected the following input types: audio-visual, visual only, and audio only, for every 45 epochs in the training phase. When using the visual input only with the audio input set to zeros, the visual output was provided while audio output was set upon two different models: Model-1 set the audio target to zeros; Model-2 used the clean audio as the target. Similarly, when using the audio only data with the visual input set to zeros, Model-1 set the visual target to zeros, and Model-2 used the original visual data for the visual target. Please note that both Model-1 and Model-2 are trained via the multi-style training strategy, and the difference is the information specified in the output during the training process. The mean square error (MSE) from the training processes of Model-I and Model-II are listed in Figs. 14 and 15. On the tops of Figs. 14 and 15, we used the bars to mark the epoch segments of the three types of input, including audio-visual, visual only, and audio only.

From the results of Figs. 14 and 15, we have observed something supportive for adding visual information. In the windows with solid red line of these two figures, we note that the audio loss is relatively large when we use audio only data for training; the MSE dropped to a lower level once visual features are used, indicating the strong correlation of audio and visual streams. Besides, in the dotted red window in Fig. 15, an acceptable audio loss could be obtained even when the model was trained with visual data only, which inspired us to perform a simple speech synthesis experiment with visual data only using our model architecture. The results will be further discussed in Section IV-G.

#### E. Mixing Weight

In the above experiments, the mixing weight in Eq. (5) was fixed to 1. Namely, the errors are considered equally when training the model parameters of AVDCNN. In this sub-section, we intended to explore the correlation of  $\mu$  to the SE performance. Fig. 16 shows the audio and visual losses in the training data under different mixing weights during the training process of the AVDCNN model. It is observed that the more we emphasized on the visual information, i.e., the larger value of mixing weight  $\mu$ , the better visual loss and the worse audio loss we got. Given that the audio loss dominated the enhancement results, we tend to select a smaller  $\mu$ .

#### F. Multimodal Inputs with Mismatched Visual Features

In this sub-section, we show the importance of correct matching between input audio features with its visual counterpart features. We selected eight shapes of mouth during speech as stationary visual units, and then for each “snapshot”, we fixed it as visual features for the entire utterance. From the spectrogram in Fig. 17, we can see that the AVDCNN enhanced speech with correct lip features preserves more detailed structures than other enhanced speech signals with incorrect lip sequences. The mean

PESQ score of 40 testing utterances with correct visual features is 2.54, and the mean score of enhanced speech signals with the eight fake lip shape sequences range from 1.17 to 2.07. The results suggest that the extraction of lip shape notably affects the performance of AVDCNN.

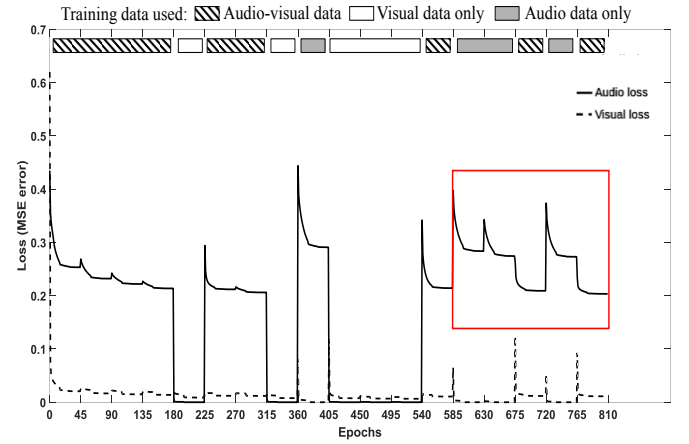


Fig. 14 The learning curve of the training data of the multi-style learning model, Model-I: set visual/audio target to zeros when only audio/visual input is selected in training. The red frame shows a smaller audio loss can be obtained as additional visual information is included.

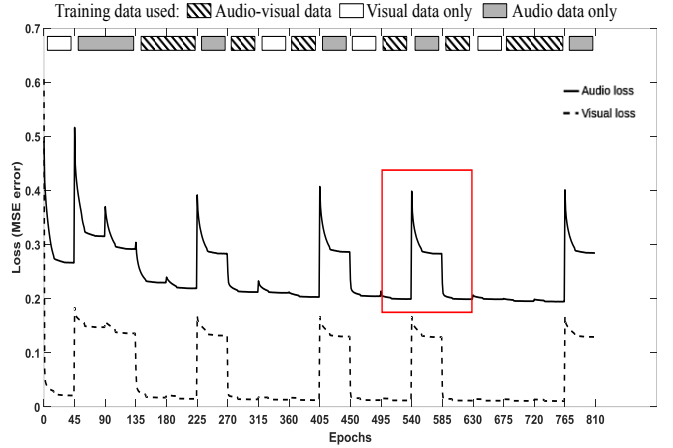


Fig. 15 The learning curve of the training data of the multi-style learning model, Model-II: remain visual/audio target when only audio/visual input is selected in training. The red frame shows a smaller audio loss can be obtained as additional visual information is included.

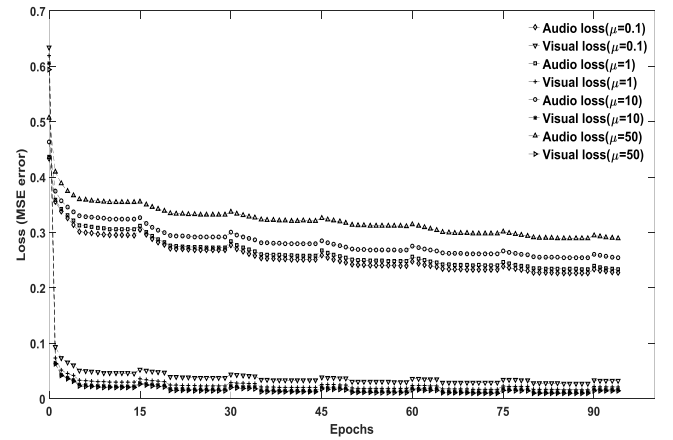


Fig. 16 Audio and visual losses in the training data under different mixing weights during the training process of the AVDCNN model.

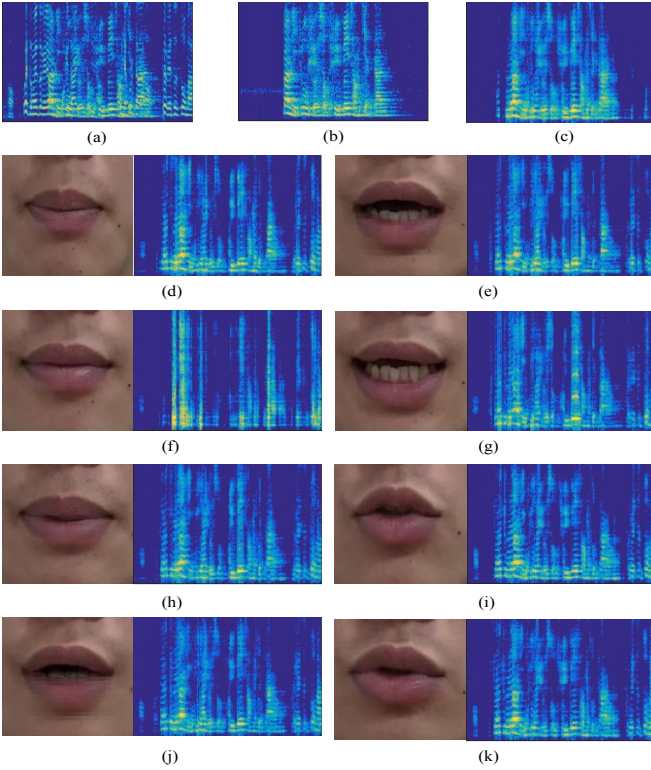


Fig. 17 (a) Noisy speech of 1T(on-air) at 0 dB SIR, (b) clean speech, (c)AVDCNN enhanced speech with correct lip features, (d)-(k) (left) selected lip shape, (right) AVDCNN enhanced speech with incorrect lip features, which are sequences of the selected lip shape.

#### G. Reconstructed Mouth Images

In the proposed AVDCNN system, we use visual input as an auxiliary clue for speech signals and add visual information at output as a part of the constraints during the training of the model. Therefore, the proposed system is actually an audio-visual encoder-decoder system with multi-task learning. In addition to enhanced speech frames, we receive the corresponding mouth images at the output in the testing phase. It is interesting to investigate the images obtained using the audio-visual encoder-decoder system. Fig. 19 shows a few visualized samples. For now, we simply view these images as a “by-product” of the audio-visual system, compared with the target enhanced speech signals. However, in the future, it will be interesting to explore the lip shape that the model learns when the corresponding fed visual hints are considerably corrupted or not provided.

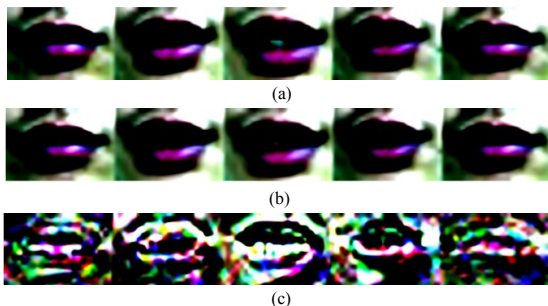


Fig. 18 Visualizing the normalized mouth images. (a) Visual input and (b) visual output of the proposed AVDCNN model. (c) Difference between (a) and (b), with amplitude magnified ten times.

#### H. Subjective Listening Tests

In addition to instrumental evaluations, we also conducted subjective listening tests for enhanced speech from three different methods, including logMMSE, ADCNN, and AVDCNN. We referred the procedures of listening tests in [76], using five-point scale to evaluate background noise intrusiveness (BAK) and overall effect (OVRL). Higher point is more favorable. Each subject listened to 10 utterances enhanced from all 10 testing noises under -5dB SIR and -5dB SAR by the aforementioned three models, resulting in a total of  $(3 \times 10 \times 10)$  utterances. 20 subjects, whose native language is Mandarin, participated in the test. The subjects were aged from 23 to 40 years, with a mean of 26 years. The mean scores over subjects are shown in Table II. The results showed that the proposed AVDCNN model obtained the best scores among the three models compared in the subjective listening tests.

TABLE II

RESULTS OF THE SUBJECTIVE LISTENING TESTS

Models	BAK	OVRL
LogMMSE	1.20	1.70
ADCNN	2.75	1.95
AVDCNN	<b>3.70</b>	<b>2.95</b>

#### I. Early Fusion Scheme for the AVDCNN Model

We also tried the early fusion scheme by combining audio and visual features at inputs before entering the convolutional layers. The early fusion model, denoted by AVDCNN-EF, replaced Audio Network and Visual Network in Fig. 1 with united CNNs, whose input is the fused audio-visual feature generated by concatenating audio features, separated RGB channels of visual features, and zero paddings with a final shape of  $257 \times 29 \times 1$  (audio: $257 \times 5 \times 1$ , RGB: $(80+80+80) \times 24 \times 1$ , and zero padding: $17 \times 24 \times 1$ ). Numbers of parameters of AVDCNN and AVDCNN-EF are at the same order. The comparison of instrumental metrics of enhanced results by the AVDCNN and AVDCNN-EF models are shown in Table III. The scores are the mean scores of enhanced speech over 10 different noises under different SIRs at SAR 0dB. It is clear that AVDCNN consistently outperforms AVDCNN-EF, indicating that the proposed fusion scheme, which processes audio and visual information individually first and fuses them later, is better than an early fusion scheme that combines the heterogeneous data in the beginning.

#### J. Comparison with Other Audio-Visual SE Model

In this sub-section, we compared the AVDCNN model with the audio-visual SE model in [49], denoted by AVDNN. The AVDNN model used hand-crafted audio and visual features, which are Mel-filter banks and mutual distance change between points in lip contour, respectively. Other main differences between AVDCNN and AVDNN are that the AVDNN model is based on DNN and does not adopt the multi-tasking learning scheme, while AVDCNN applies multi-task learning by considering audio and visual information at the output layer.

The spectrogram of enhanced speech by AVDCNN and AVDNN is shown in Fig. 19. Comparing AVDNN-enhanced speech with AVDCNN-enhanced speech, we noticed that AVDNN could not effectively remove background noise in the non-speech segment, suggesting that the visual features learned

by CNNs directly from images could be more robust than the hand-crafted features used in AVDNN. In [49], the testing condition was a noise-matched scenario, which was much less challenging than the testing condition in the present study. As shown in Fig. 19, under the noise-mismatched testing scenario, the AVDNN model could not reconstruct the target speech as effectively as the AVDCNN model. We also listed the mean scores of instrumental metrics of AVDNN in Table III for comparison. The results show that AVDCNN consistently outperforms AVDNN in all metrics. The results in Table III demonstrate that the proposed AVDCNN model outperforms the other two audio-visual SE models.

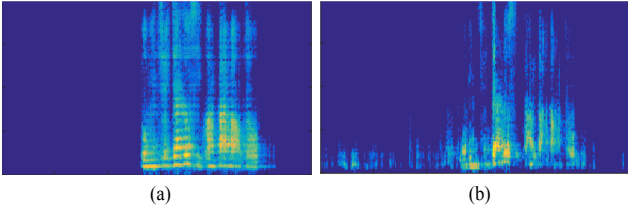


Fig. 19 Spectrograms of enhanced speech for noisy speech with music at 5dB SIR and ambient noise at 5dB SAR by (a) AVDCNN and (b) AVDNN.

TABLE III

MEAN SCORES OF INSTRUMENTAL METRICS OF ENHANCED SPEECH OVER 10 DIFFERENT NOISES UNDER DIFFERENT SIRS AT 0 dB SAR FOR EACH AUDIO-VISUAL SE MODELS

Models	PESQ	STOI	SDI	HASQI	HASPI
AVDCNN	<b>2.41</b>	<b>0.66</b>	<b>0.45</b>	<b>0.43</b>	<b>0.99</b>
AVDCNN-EF	1.52	0.51	1.43	0.11	0.74
AVDNN	1.65	0.50	0.96	0.08	0.45

## V. DISCUSSION

From the previous experiments, we can observe clear evidence in how visual information can affect the enhancement results. For instance, Fig. 3, (f) shows that noise and speech signals from non-targeted speaker are effectively suppressed when mouth is closed. The result indicated that the visual information plays a beneficial role in voice activity detection (VAD). Actually, there are researchers working on this particular direction [77, 78]. This is also part of the reason why we choose in-car environments as our testing scenario and investigate the effectiveness of audio-visual SE. If there is a camera that targets on driver's mouth region, lip shape could be a strong hint on whether or not to activate a voice command system with background talkers or noises, and in addition, enhance the speech. Lip shape could be a useful hint for VAD; however, it does not seem a very solid one yet. In a few testing results of enhanced speech by the AVDCNN model, as shown in Fig. 20, we observed noise components were removed incompletely in the non-speech segment due to the open shape of the mouth at the time. We think this shortcoming could be further improved with the combination of audio-only VAD techniques.

We also preliminarily evaluated the AVDCNN model on real-world testing data, i.e., the noisy speech was recorded in a real noisy environment rather than artificially adding noise to the clean speech. Fig. 21 (a) shows the controlled environment for recording training and testing data. Fig. 21 (b) shows the recording condition of the real-world data, which was recorded

by a smart phone (ASUS ZenFone 2 ZE551ML) in a night market. Spectrograms of noisy and AVDCNN-enhanced speech signals are shown in Fig. 21 (c) and (d), respectively. The red frame indicates the segment when the target speech is mixed with background talking sound. We observed that the lip shape helped identifying the target speech segment, while the reconstruction on target speech was not as good as the enhanced results in the controlled environment. This might be due to different light coverage, a lower SIR, or properties of the background noise, suggesting there is still room for improvement in audio-visual SE in real-word testing conditions.

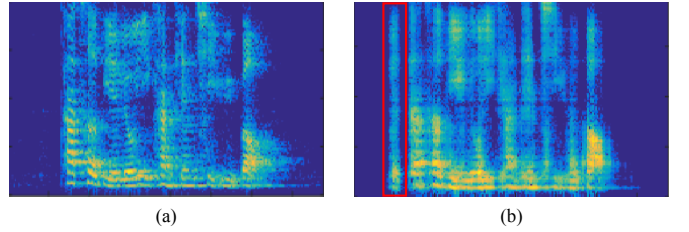


Fig. 20 Spectrograms of (a) clean speech and (b) AVDCNN enhanced speech. Red frame in (b) shows that noise is reduced incompletely in the non-speech segment if the mouth is in an unclosed shape.

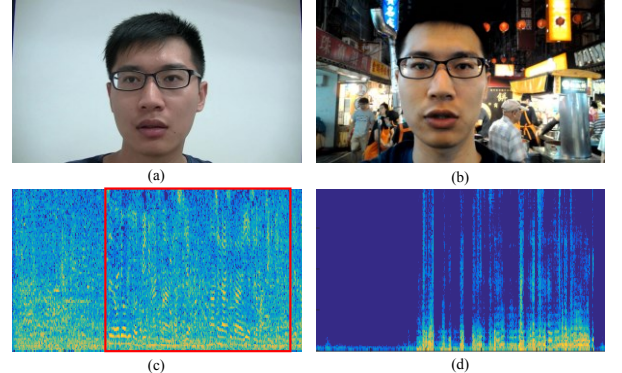


Fig. 21 Tests in real-world conditions. (a) The controlled environment (seminar room) for recording training and testing data. (b) Recording environment (night market) for real-world test data. Spectrograms of (c) noisy speech with babble noise and (d) enhanced speech by the AVDCNN model. Red frame in (c) indicates the segment when the target speech was mixed with noise.

## VI. CONCLUSION

In this paper, we have proposed a novel CNN-based audio-visual encoder-decoder system with multi-task learning, called AVDCNN, for speech enhancement. The model utilizes individual networks to process input data with different modalities, and a fusion network is followed to learn joint multimodal features. We train the model in an end-to-end manner. The experimental results obtained using the proposed architecture show that its performance in the SE task is better than that of three audio-only baseline models in terms of five instrumental evaluation metrics, confirming the effectiveness of integrating visual information with audio information into the SE process. We also show its effectiveness by comparing to other audio-visual SE models. Overall, the contributions of this paper are five-fold. First, we adopted CNNs for audio and visual streams in the proposed end-to-end audio-visual SE model with improvements over many baseline models. Second, we denoted the advantages

of integrating visual information in SE through the multi-modal and multi-task training strategies. Third, we demonstrated that processing audio and visual streams with late fusion is better than early fusion. Fourth, the experimental results exhibited the highly correlation of speech and lip shape, and the importance of using correct lip shape in audio-visual SE. Finally, we showed lip shape is effective as auxiliary features in VAD and also pointed out the potential problems when using it. In the future, we will try to improve the proposed architecture by using a whole face as visual input rather than mouth region only, in order to exploit well-trained face recognition networks for improving visual descriptor networks. Also, we plan to modify existing CNNs in our model by targeting on other state-of-the-art CNN-based models, such as fully convolutional networks [79] and U-Net [80]. Lastly, to improve the practicability of the model in real-world application scenario, collecting training data including more complicated and real conditions are considered.

#### ACKNOWLEDGMENT

This work was supported by the Academia Sinica Thematic Research Program AS-105-TP-C02-1.

#### REFERENCES

- [1] J. Li, L. Deng, R. Haeb-Umbach, and Y. Gong, *Robust Automatic Speech Recognition: A Bridge to Practical Applications*, 1st ed. Academic Press, 2015.
- [2] B. Li, Y. Tsao, and K. C. Sim, “An investigation of spectral restoration algorithms for deep neural networks based noise robust speech recognition,” in *Proc. INTERSPEECH*, 2013, pp. 3002–3006.
- [3] A. El-Solh, A. Cuhadar, and R. A. Goubran, “Evaluation of speech enhancement techniques for speaker identification in noisy environments,” in *Proc. ISMW*, 2007, pp. 235–239.
- [4] J. Ortega-Garcia and J. Gonzalez-Rodriguez, “Overview of speech enhancement techniques for automatic speaker recognition,” in *Proc. ICSLP*, vol. 2, 1996, pp. 929–932.
- [5] J. Li, L. Yang, Y. Hu, M. Akagi, P.C. Loizou, J. Zhang, and Y. Yan, “Comparative intelligibility investigation of single-channel noise reduction algorithms for Chinese, Japanese and English,” *Journal of the Acoustical Society of America*, vol. 129, no. 5, pp. 3291–3301, 2011.
- [6] J. Li, S. Sakamoto, S. Hongo, M. Akagi, and Y. Suzuki, “Two-stage binaural speech enhancement with Wiener filter for high-quality speech communication,” *Speech Communication*, vol. 53, no. 5, pp. 677–689, 2011.
- [7] T. Venema, *Compression for Clinicians*, 2nd ed. Thomson Delmar Learning, 2006, ch. 7.
- [8] H. Levitt, “Noise reduction in hearing aids: an overview,” *J. Rehab. Res. Dev.*, vol. 38, no. 1, pp. 111–121, 2001.
- [9] Y.-H. Lai, F. Chen, S.-S. Wang, X. Lu, Y. Tsao, and C.-H. Lee, “A deep denoising autoencoder approach to improving the intelligibility of vocoded speech in cochlear implant simulation,” *IEEE Transactions on Biomedical Engineering*, vol. 64, no. 7, pp. 1568–1578, 2016.
- [10] F. Chen, Y. Hu, and M. Yuan, “Evaluation of noise reduction methods for sentence recognition by Mandarin-speaking cochlear implant listeners,” *Ear and Hearing*, vol. 36, no. 1, pp. 61–71, 2015.
- [11] J. Chen, “Fundamentals of Noise Reduction,” in *Spring Handbook of Speech Processing*, Springer, 2008, ch. 43.
- [12] P. Scalart and J. V. Filho, “Speech enhancement based on a priori signal to noise estimation,” in *Proc. ICASSP*, 1996, pp. 629–632.
- [13] Y. Ephraim and D. Malah, “Speech enhancement using a minimum mean-square error short-time spectral amplitude estimator,” *IEEE Transactions on Acoustics, Speech and Signal Processing*, vol. 32, no. 6, pp. 1109–1121, 1984.
- [14] R. Martin, “Speech enhancement based on minimum mean-square error estimation and supergaussian priors,” *IEEE Transactions on Speech and Audio Processing*, vol. 13, no. 5, pp. 845–856, 2005.
- [15] Y. Tsao and Y.-H. Lai, “Generalized maximum a posteriori spectral amplitude estimation for speech enhancement,” *Speech Communication*, vol. 76, pp. 112–126, 2015.
- [16] A. Hussain, M. Chetouani, S. Squartini, A. Bastari, and F. Piazza, “Nonlinear speech enhancement: An overview,” in *Progress in Nonlinear Speech Processing*. Berlin, Germany: Springer, 2007, pp. 217–248.
- [17] A. Uncini, “Audio signal processing by neural networks”, *Neurocomputing*, vol. 55, pp. 593–625, 2003.
- [18] G. Cocchi and A. Uncini, “Subband neural networks prediction for on-line audio signal recovery,” *IEEE Transactions on Neural Networks*, vol. 13, no. 4, pp. 867–876, 2002.
- [19] N. B. Yoma, F. McInnes, M. Jack, “Lateral inhibition net and weighted matching algorithms for speech recognition in noise,” *Proc. IEE Vision, Image & Signal Processing*, vol. 143, no. 5, pp. 324–330, 1996.
- [20] X. Lu, Y. Tsao, S. Matsuda, and C. Hori, “Speech enhancement based on deep denoising autoencoder,” in *Proc. INTERSPEECH*, 2013, pp. 436–440.
- [21] X. Lu, Y. Tsao, S. Matsuda, and C. Hori, “Ensemble modeling of denoising autoencoder for speech spectrum restoration,” in *Proc. INTERSPEECH*, 2014, pp. 885–889.
- [22] Y. Xu, J. Du, L.-R. Dai, and C.-H. Lee, “An experimental study on speech enhancement based on deep neural networks,” *IEEE Signal Processing Letters*, vol. 21, pp. 65–68, 2014.
- [23] D. Liu, P. Smaragdis, and M. Kim, “Experiments on deep learning for speech denoising,” in *Proc. INTERSPEECH*, 2014, pp. 2685–2689.
- [24] M. Kolbæk, Z.-H. Tan, and J. Jensen, “Speech intelligibility potential of general and specialized deep neural network based speech enhancement systems,” *IEEE/ACM Transactions on Audio, Speech, and Language Processing*, vol. 25, pp. 153–167, 2017.
- [25] F. Weninger, F. Eyben, and B. Schuller, “Single-channel speech separation with memory-enhanced recurrent neural networks,” in *Proc. ICASSP*, 2014, pp. 3709–3713.
- [26] F. Weninger, H. Erdogan, S. Watanabe, E. Vincent, J. L. Roux, J. R. Hershey, and B. Schuller, “Speech enhancement with LSTM recurrent neural networks and its application to noise-robust ASR,” in *Latent Variable Analysis and Signal Separation*, pp. 91–99. Springer, 2015.
- [27] P. Campolucci, A. Uncini, F. Piazza, and B. Rao, “On-line learning algorithms for locally recurrent neural networks,” *IEEE Transactions on Neural Networks*, vol. 10, no. 2, pp. 253–271, 1999.
- [28] F. Eyben, F. Weninger, S. Squartini, and B. Schuller, “Real-life voice activity detection with LSTM recurrent neural networks and an application to Hollywood movies,” in *Proc. ICASSP*, 2013, pp. 483–487.
- [29] S.-W. Fu, Y. Tsao, and X. Lu, “SNR-Aware convolutional neural network modeling for speech enhancement,” in *Proc. INTERSPEECH*, 2016.
- [30] S.-W. Fu, Y. Tsao, and X. Lu, “Complex spectrogram enhancement by convolutional neural network with multi-metrics learning,” in *Proc. MLSP*, 2017.
- [31] H. McGurk and J. MacDonald, “Hearing lips and seeing voices,” *Nature*, vol. 264, pp. 746–748, 1976.
- [32] D. G. Stork and M. E. Hennecke, *Speechreading by Humans and Machines*, Springer, 1996.
- [33] G. Potamianos, C. Neti, G. Gravier, A. Garg, and Andrew W, “Recent advances in the automatic recognition of audio-visual speech,” *Proceedings of IEEE*, vol. 91, no. 9, 2003.
- [34] D. Kolossa, S. Zeiler, A. Vorwerk, and R. Orglmeister, “Audiovisual speech recognition with missing or unreliable data,” in *Proc. AVSP*, 2009, pp. 117–122.
- [35] A. V. Neffan, L. Liang, X. Pi, X. Liu, and K. Murphy, “Dynamic Bayesian networks for audio-visual speech recognition,” *EURASIP Journal on Applied Signal Processing*, vol. 2002, no. 11, pp. 1274–1288, 2002.
- [36] A. H. Abdelaziz, S. Zeiler, and D. Kolossa, “Twin-HMM-based audio-visual speech enhancement,” in *Proc. ICASSP*, 2013, pp. 3726–3730.
- [37] S. Deligne, G. Potamianos, and C. Neti, “Audio-visual speech enhancement with AVCDCN (audio-visual codebook dependent cepstral normalization),” in *Proc. Int. Conf. Spoken Lang. Processing*, 2002, pp. 1449–1452.
- [38] H. Meutner, N. Ma, R. Nickel, C. Schymura, and D. Kolossa, “Improving audio-visual speech recognition using deep neural networks with dynamic stream reliability estimates,” in *Proc. ICASSP*, 2017.
- [39] V. Estellers, M. Gurban, and J.-P. Thiran, “On dynamic stream weighting for audio-visual speech recognition,” *IEEE Transactions on Audio, Speech, and Language Processing*, vol. 20, no. 4, pp. 1145–1157, 2012.

[40] J. Ngiam, A. Khosla, M. Kim, J. Nam, H. Lee, and A. Ng, "Multimodal deep learning," in *Proc. ICML*, 2011.

[41] Y. Mroueh, E. Marcheret, and V. Goel, "Deep multimodal learning for audio-visual speech recognition," in *Proc. ICASSP*, 2015.

[42] L. Girin, J.-L. Schwartz, and G. Feng, "Audio-visual enhancement of speech in noise," *Journal of the Acoustical Society of America*, vol. 109, pp. 3007, 2001.

[43] R. Goecke, G. Potamianos, and C. Neti, "Noisy audio feature enhancement using audio-visual speech data," in *Proc. ICASSP*, 2002.

[44] I. Almajai and B. Milner, "Enhancing audio speech using visual speech features," in *Proc. INTERSPEECH*, 2009.

[45] I. Almajai and B. Milner, "Visually derived Wiener filters for speech enhancement," *IEEE Transactions on Audio, Speech, and Language Processing*, vol. 19, no. 6, pp. 1642–1651, 2011.

[46] B. Rivet, L. Girin, and C. Jutten, "Visual voice activity detection as a help for speech source separation from convolutive mixtures," *Speech Communication*, vol. 49, no. 7-8, pp. 667–677, 2007.

[47] B. Rivet, L. Girin, and C. Jutten, "Mixing audiovisual speech processing and blind source separation for the extraction of speech signals from convolutive mixtures," *IEEE Transactions on Audio, Speech, and Language Processing*, vol. 15, no. 1, pp. 96–108, 2007.

[48] B. Rivet, W. Wang, S. M. Naqvi, and J. A. Chambers, "Audiovisual speech source separation: An overview of key methodologies," *IEEE Signal Processing Magazine*, vol. 31, no. 3, pp. 125–134, May 2014.

[49] J.-C. Hou, S.-S. Wang, Y.-H. Lai, J.-C. Lin, Y. Tsao, H.-W. Chang, and H.-M. Wang, "Audio-visual speech enhancement using deep neural networks," in *Proc. APSIPA ASC*, 2016.

[50] G. Tzimiropoulos and M. Pantic, "Gauss-Newton deformable part models for face alignment in-the-wild," in *Proc. CVPR*, 2014, pp. 1851–1858.

[51] Z. Wu, S. Sivadas, Y. K. Tan, B. Ma, and S. M. Goh, "MultiModal hybrid deep neural network for speech enhancement," *arXiv preprint arXiv:1606.04750*, 2016.

[52] K. Simonyan and A. Zisserman, "Very deep convolutional networks for large-scale image recognition," in *Proc. ICLR*, 2015.

[53] O. M. Parkhi, A. Vedaldi, and A. Zisserman, "Deep face recognition," in *Proc. BMVC*, 2015.

[54] A. W. Rix, J. G. Beerends, M. P. Hollier, and A. P. Hekstra, "Perceptual evaluation of speech quality (PESQ) – a new method for speech quality assessment of telephone networks and codecs," in *Proc. ICASSP*, 2001.

[55] C. Taal, R. Hendriks, R. Heusdens, and J. Jensen, "An algorithm for intelligibility prediction of time-frequency weighted noisy speech," *IEEE Transactions on Acoustics, Speech and Signal Processing*, vol. 19, pp. 2125–2136, 2011.

[56] J. Chen, J. Benesty, Y. Huang, and S. Doclo, "New insights into the noise reduction Wiener filter," *IEEE/ACM Transactions on Audio, Speech, and Language Processing*, vol. 14, pp. 1218–1234, 2006.

[57] J. M. Kates and K. H. Arehart, "The hearing-aid speech quality index (HASPI)," *Journal of the Audio Engineering Society*, vol. 58, no. 5, pp. 363–381, 2010.

[58] J. M. Kates and K. H. Arehart, "The hearing-aid speech perception index (HASPI)," *Speech Communication*, vol. 65, pp. 75–93, 2014.

[59] M. W. Huang, "Development of Taiwan Mandarin hearing in noise test," Master thesis, Department of speech language pathology and audiology, National Taipei University of Nursing and Health science, 2005.

[60] P. Viola and M. J. Jones, "Robust Real-Time Face Detection," *International Journal of Computer Vision*, vol. 57, no. 2, pp. 137–154, 2004.

[61] R. Caruana, "Multitask learning," *Machine learning*, vol. 28, pp. 41–75, 1997.

[62] M. L. Seltzer and J. Droppo, "Multi-task learning in deep neural networks for improved phoneme recognition," in *Proc. ICASSP*, 2013, pp. 6965–6969.

[63] A. Rezayee, and S. Gazor, "An adaptive KLT approach for speech enhancement," *IEEE Transactions on Speech and Audio Processing*, vol. 9, no. 2, pp. 87–95, 2001.

[64] Y. Ephraim, and D. Malah, "Speech enhancement using a minimum mean-square error log-spectral amplitude estimator," *IEEE Transactions on Acoustics, Speech and Signal Processing*, vol. 33, no. 2, pp. 443–445, 1985.

[65] E. Principi, S. Cifani, R. Rotili, S. Squartini, F. Piazza, "Comparative evaluation of single-channel mmse-based noise reduction schemes for speech recognition," *Journal of Electrical and Computer Engineering*, pp. 1–7, 2010.

[66] J. Hong, S. Park, S. Jeong, and M. Hahn, "Dual-microphone noise reduction in car environments with determinant analysis of input correlation matrix," *IEEE Sensors Journal*, vol. 16, no. 9, pp. 3131–3140, 2016.

[67] Y. Xu, J. Du, L.-R. Dai, and C.-H. Lee, "A regression approach to speech enhancement based on deep neural networks," *IEEE/ACM Transactions on Audio, Speech and Language Processing*, vol. 23, no. 1, pp. 7–19, 2015.

[68] G. Hu, 100 nonspeech environmental sounds, 2004 [Online]. Available: <http://web.cse.ohio-state.edu/pnl/corpus/HuNonspeech/HuCorpus.html>.

[69] B. Lee, M. Hasegawa-Johnson, C. Goudeseune, S. Kamdar, S. Borys, M. Liu, and T. Huang, "AVICAR: Audio-visual speech corpus in a car environment," in *Proc. Int. Conf. Spoken Language*, 2004, pp. 2489–2492.

[70] P. C. Loizou, *Speech Enhancement: Theory and Practice*, 2nd ed., Boca Raton, FL, USA: CRC, 2013.

[71] G. Hinton, N. Srivastava, and K. Swersky, "Lecture 6: Overview of mini-batch gradient descent," Coursera Lecture slides <https://class.coursera.org/neuralnets-2012-001/lecture>.

[72] F. Chollet. (2015). *Keras*. Available: <https://github.com/fchollet/keras>

[73] J. W. Tukey, "Comparing individual means in the analysis of variance," *Biometrics*, vol. 5, no. 2, pp. 99–114, 1949.

[74] C. Feichtenhofer, A. Pinz, and A. Zisserman, "Convolutional two-stream network fusion for video action recognition," in *Proc. CVPR*, 2016.

[75] J. S. Chung, A. Senior, O. Vinyals, and A. Zisserman, "Lip reading sentences in the wild," *arXiv preprint arXiv:1611.05358*, 2016.

[76] S. Ntalampiras, T. Ganchev, I. Potamitis, and N. Fakotakis, "Objective comparison of speech enhancement algorithms under real world conditions," in *Proc. PETRA*, 2008.

[77] S. Thermos, and G. Potamianos, "Audio-visual speech activity detection in a two-speaker scenario incorporating depth information from a profile or frontal view," in *Proc. SLT*, 2016.

[78] F. Patrona, A. Iosifidis, A. Tefas, N. Nikolaidis, and I. Pitas, "Visual voice activity detection in the wild," *IEEE Transactions on Multimedia*, vol. 18, no. 6, pp. 967–977, 2016.

[79] J. Long, E. Shelhamer, and T. Darrell, "Fully convolutional networks for semantic segmentation," in *Proc. CVPR*, 2015.

[80] O. Ronneberger, P. Fischer, and T. Brox, "U-Net: convolutional networks for biomedical image segmentation," in *Proc. MICCAI*, 2015.